The Comprehensive Subcortical and Cerebellar Atlas of the Human Brain using multimodal MRI at 7T.

Kadharbatcha S Saleem[1], Alexandru V Avram[1], Daniel Glen[2], Cecil Chern-Chyi Yen[3], and Peter J Basser[1]

[1]Section on Quantitative Imaging and Tissue Sciences (SQITS), Eunice Kennedy Shriver National Institute of Child Health and Human Development (NICHD), NIH, Bethesda, MD 20892; [2]Scientific and Statistical Computing Core, National Institute of Mental Health (NIMH), NIH, Bethesda, MD 20892; [3]Neurophysiology Imaging Facility, National Institute of Mental Health (NIMH), NIH, Bethesda, MD 20892.

1746

Introduction

The thalamus, basal ganglia, brainstem nuclei, and other subcortical regions regulate autonomic, sensorimotor, cognitive, and limbic functions. In primates, high-resolution mapping of these subcortical regions using a comprehensive 3D digital atlas based on multimodal MRI[1,2] has proven remarkably useful in anatomical, functional, and clinical studies. In particular, registering a 3D atlas to a given human brain MRI scan is immediately valuable for determining regions of interest for various applications, including tractography studies, the areal location of fMRI responses, and potential targets for deep brain stimulation (DBS) in neurological disorders. This study developed a subcortical and cerebellar atlas of the human brain in 3D using ultra-high-resolution mean apparent propagator (MAP)-MRI[3,4], MTR, and T2W images.

Methods

We dissected the entire human brainstem, along with the thalamus and basal ganglia, but excluded the cerebellum (**Fig. 1A**), from a postmortem, formalin-fixed adult female brain (age: 24 years; PMI: 34 hr; fixation time: over six months). The brainstem block was immersed in 0.1M PBS-saline containing sodium azide prior to MRI data acquisition. The specimen was placed in a custom-made mold and container assembly (**Fig. 1B-D**) and scanned on a 7T scanner using MAP-MRI at a resolution of 250 µm. We acquired 104 DWIs with multiple b-values (bmax=10000 s/mm2), and the pulse duration and separation were δ=8 ms and Δ=28 ms, respectively. In each voxel, we estimated the MAP and calculated the microstructural DTI/MAP parameters: fractional anisotropy (FA); mean, axial, and radial diffusivities (MD, AD, and RD, respectively); propagator anisotropy (PA), non-Gaussianity (NG), return-to-origin probability (RTOP), return-to-axis probability (RTAP), and return-to-plane probability (RTPP), along with the fiber orientation distribution (FOD) functions. We computed the MT ratio (MTR) from 3D gradient echo images obtained with and without MT preparation. The total duration of the MAP-MRI scan was 62 h and 25 min, while the MT scan lasted 13 h and 7 min.

Using AFNI's[6] sswarper[7] for nonlinear alignment, the ex vivo MAP-MRI dataset was registered to the in vivo 2009b MNI_icbm152 template[8]. We also registered the direction-encoded color (DEC) volume derived from the in vivo human whole-brain connectome diffusion MRI (dMRI) and the BigBrain dataset to the same MNI volume[9,10]. All these volumes registered well to the standard MNI space (**Fig. 2A-F**), enabling us to delineate different subcortical nuclei and white matter fiber tracts directly on the MNI template. Guided by an in vivo whole-brain connectome dMRI and the BigBrain dataset with the MNI 2009b template, we also delineated a new human cerebellar atlas called "HCA" (**Figs. 6-8**).

Brainstem specimen, and MR imaging assembly

Fig. 1

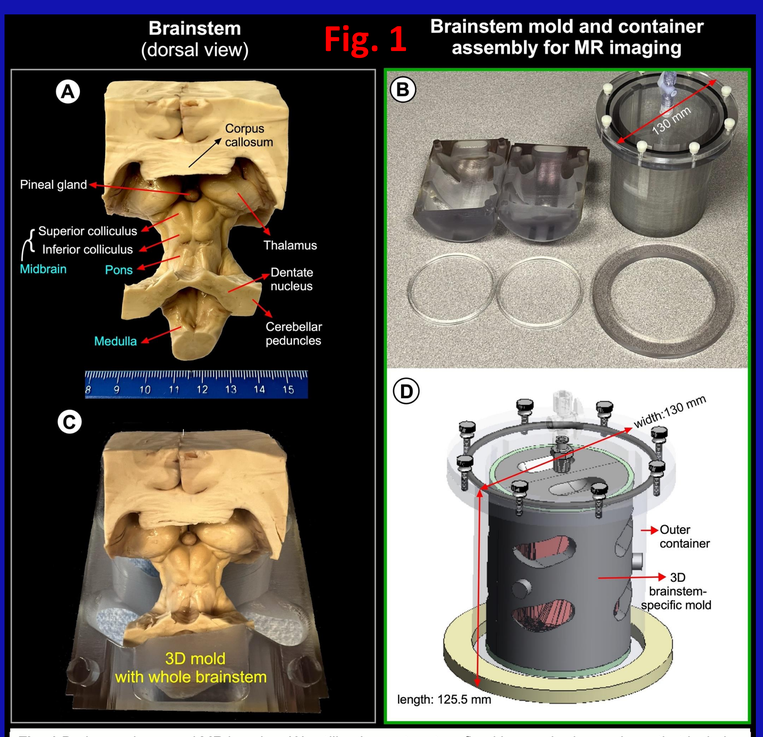

Fig. 1 Brain specimen and MR imaging. We utilized a postmortem fixed human brain specimen that includes the entire brainstem (midbrain, pons, and medulla), thalamus, and basal ganglia (**A**). The cerebellum is detached from the brainstem, leaving only the cerebellar peduncles visible. We constructed a brainstem-specific mold using a container assembly (diameter: 130 mm; **B-D**) for all MAP-MRI and MTR scans with a Bruker 7T/300 mm horizontal bore MRI scanner equipped with a 133.4 mm inner diameter RRI RFG Quadrature coil.

Ex vivo data and registration

Fig. 2

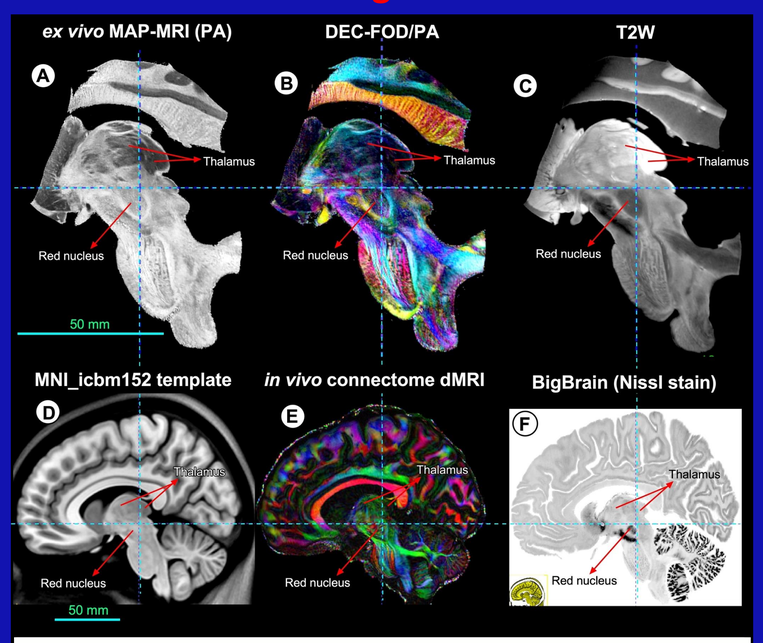

Fig. 2 Brainstem Dataset and Registration. The post-processed ex vivo MAP-MRI, combined with the T2W dataset (**A-C**), is registered to the in vivo MNI_icbm152 template (**D**). The direction-encoded color (DEC) volume, derived from the in vivo human whole-brain connectome diffusion MRI (**E**) and the BigBrain dataset (**F**), is also registered to the MNI template. It is important to note that all these volumes are well registered to the MNI. Furthermore, it is crucial to emphasize that very few regions can be delineated in the brainstem of the T1W MNI_icbm152 template itself (**D**). However, registering the ex vivo MAP-MRI (**A-C**) and DEC (**E**) volumes onto the MNI has allowed us to identify and delineate several gray matter (subcortical nuclei) and white matter fiber tracts of different orientations directly on the MNI template (see **Figs. 3F, 4C**).

Results

We identified and segmented the subregions in the basal ganglia, thalamus, hypothalamus, brainstem (midbrain, pons, and medulla), amygdala, bed nucleus of the stria terminalis, and basal forebrain directly on the in vivo MNI template using warped ex vivo MAP-MRI, T2W, and MTR images (**Fig. 3A-F**, for thalamic subregions) as references. Additionally, we segmented fiber tracts of various sizes and orientations associated with the basal ganglia, thalamus, brainstem, and cerebellum using the FOD-derived DEC map[9,11] (**Fig. 4A-F**). This newly segmented volume/template is referred to as the Subcortical Atlas of the Human Brain, or "SAHB." The SAHB atlas in **Figure 5** displays the segmented deep brain regions in 2D axial, sagittal, and coronal MRI, as well as in 3D. For the "HCA" cerebellar atlas, see **Figures 6, 7, and 8**. These digital atlases provide a practical standard reference for neuroanatomical, functional (fMRI), clinical, and connectional imaging studies.

We also validated the atlas-based area boundaries of the segmented subcortical regions by registering the HCA atlas to individual in vivo T1W MRI datasets of adult human subjects across various age groups and genders (control adults). We employed the same sswarper2[6] to align the subjects to the MNI template and inverted the combination of affine and nonlinear warps to move the HCA atlas into the subjects' native space (see **Fig. 9**). These results demonstrate that affine and nonlinear warping are sufficient to distinguish and provide atlas-based estimates of areal boundaries on individual subject-specific brain templates in vivo.

Mapping and segmentation (e.g., Thalamic subregions)

Fig. 3

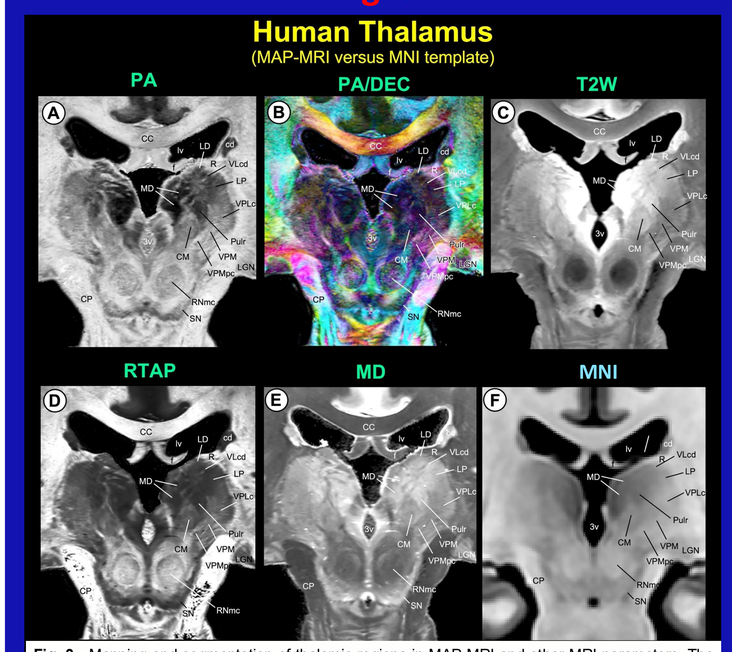

Fig. 3 Mapping and segmentation of thalamic regions in MAP-MRI and other MRI parameters. The ex vivo coronal slices at the mid-brainstem level display the subregions of the dorsal thalamus (lateral, medial, and intralaminar groups) along with surrounding areas in PA-Propagator anisotropy (**A**), PA with DEC (**B**), T2W (**C**), RTAP-return-to-axis probability (**D**), MD-medial diffusivity (**E**), and the T1W-MNI_icbm152 in vivo template (**F**). Unlike the T1W-MNI template (**F**), the various subregions of the thalamus are distinguishable through different MRI contrasts as shown in PA, T2W, RTAP, and MD (**A-E**). Additionally, the varying contrasts of the red nucleus (RNmc) in T2W and RTAP images warrant attention.

Fiber bundles (*in vivo* and *ex vivo* images)

Fig. 4

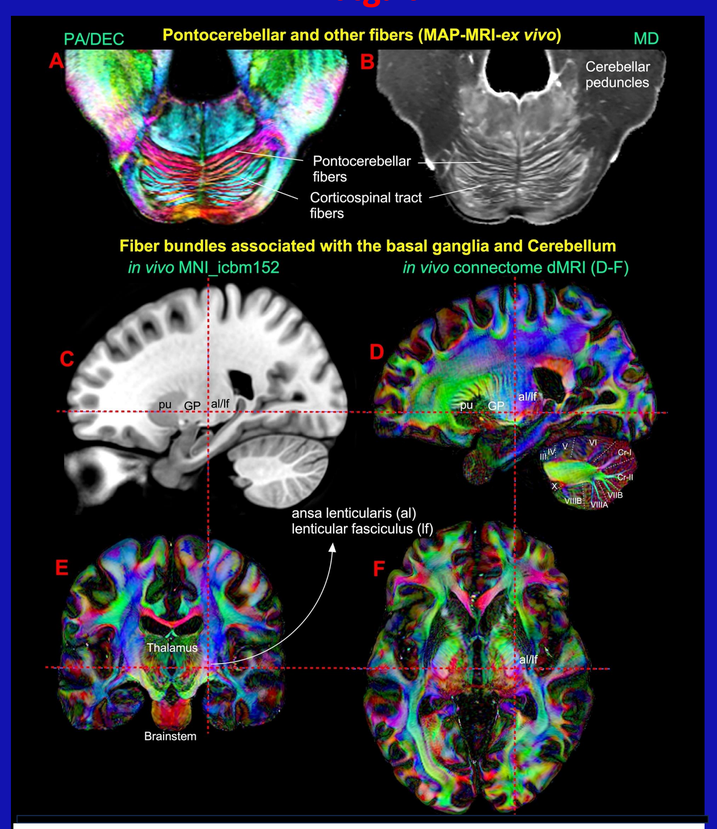

Fig. 4 Fiber bundles associated with the basal ganglia and the cerebellum in MAP-MRI and various MRI parameters. The ex vivo coronal slices at the mid-brainstem level display the mediolaterally oriented pontocerebellar fibers (red) and rostrocaudally oriented corticospinal tract (green) in PA/DEC (**A**) and MD (**B**). The fiber bundles, including the ansa lenticularis (al) and lenticular fasciculus (lf), connected to the basal ganglia and thalamus, are illustrated in vivo in the MNI template (**C**) and in vivo connectome dMRI slices (**D-F**).

Human Cerebellar Atlas ("HCA"): In 3D, Stereotaxic coordinates, and Flatmap

Fig. 6

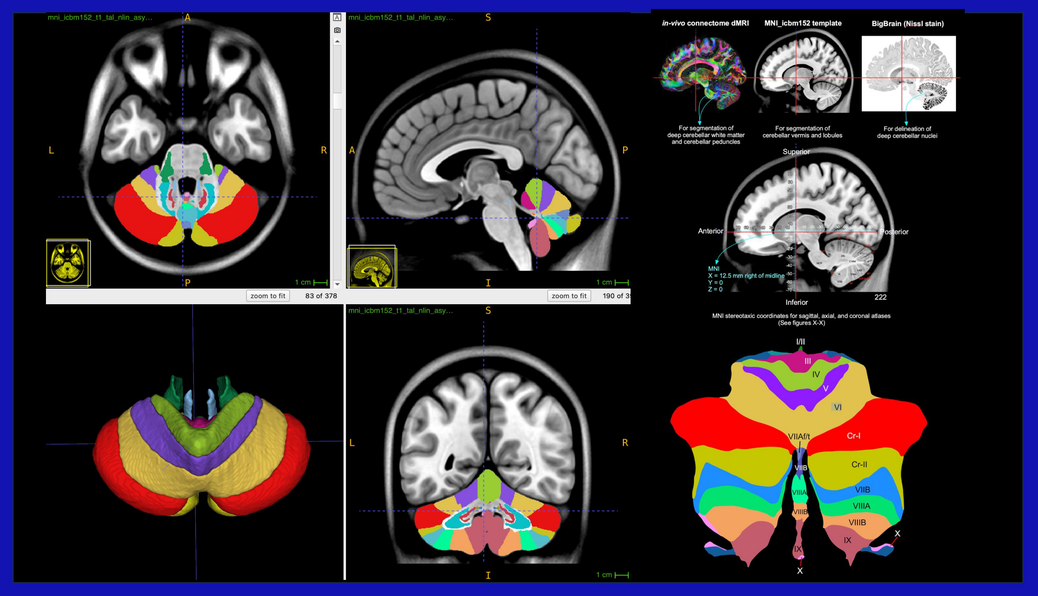

Cerebellar Atlas in coronal and sagittal planes with fiber tracts.

Figs. 7 and 8

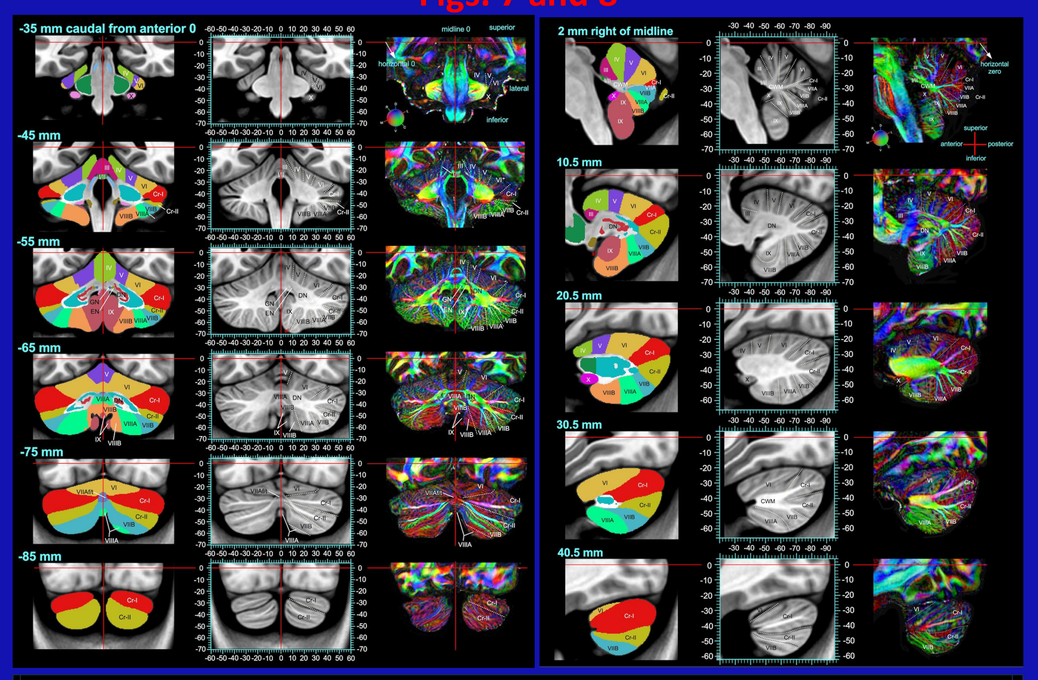

Validation of "HCA" Atlas

Fig. 9

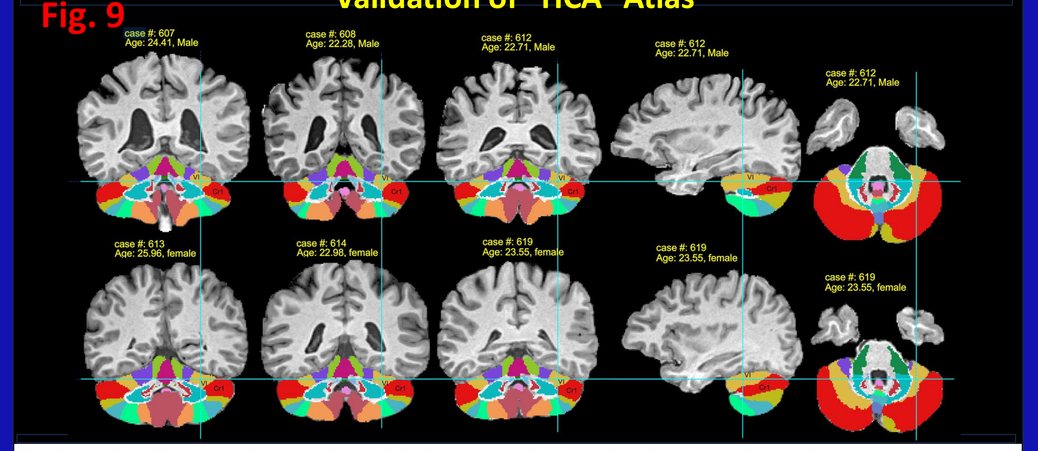

Fig. 9 Application of the Human Cerebellar Atlas ("HCA"). The cerebellar atlas is registered to in vivo control subjects across various age groups. Note that the different lobules in the cerebellar atlas (Figs. **6-8**) align well with the six registered control subjects (for example, the crosshair at Lobule VI). Cases **#612** and **#619** display the registered slices in coronal, sagittal, and axial planes.

Subcortical atlas of the Human Brain ("SAHB")

Fig. 5

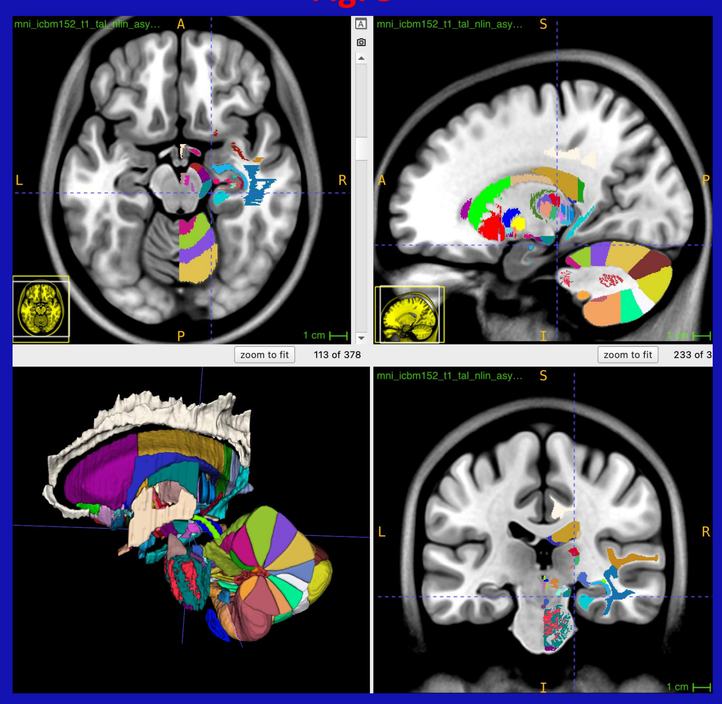

Figs. 5 and 6 Depict the subcortical atlas of the human brain ("SAHB") and the human cerebellar atlas ("HCA"), highlighting the segmented deep brain areas in the thalamus, brainstem, and various cerebellar lobules. The segmentation of these areas was performed using ITK-SNAP.

Summary and Conclusion

Using combined multimodal MRI, we developed a 3D subcortical template atlas of the entire human brainstem ex vivo and an in vivo cerebellar atlas.

The strengths of this work, compared to others, lie in its use of numerous high-resolution microstructural DTI/MAP and various MRI parameters with fODFs/DEC to segment multiple subcortical areas, including subregions of the basal ganglia, thalamus, hypothalamus, limbic regions (amygdala), basal forebrain, brainstem (midbrain, pons, and medulla), and the cerebellum.

Finally, we estimated and confirmed the atlas-based areal boundaries of subcortical regions and the cerebellum by registering the atlas templates (e.g., the HCA atlas) to in vivo T1W MRI datasets from different age groups (control adults; See Fig. 9) using a novel pipeline developed within the AFNI and SUMA software packages.

The MAP-MRI enable noninvasive segmentation of subcortical regions in the human brain. The 3D atlas provides a readily usable standard for region definition, while the template acts as a standard reference and framework.

Tracing and validating these atlas-based deep brain regions is crucial for neurosurgical planning, guiding deep brain stimulation probes, locating functional activation regions in fMRI, comparing across species, and establishing brain structure-function relationships.

References and Support:

1. Saleem KS, Avram AV, Glen D, Yen CC, Ye FQ, Komlosh M, Basser PJ. High-resolution mapping and digital atlas of subcortical regions in the macaque monkey based on matched MAP-MRI and histology. Neuroimage. 2021; 245:118759. *https://doi.org/10.1016/j.neuroimage.2021.118759*
2. Saleem KS, Avram AV, Yen CC, Magdoom KN, Schram V, Basser PJ. Multimodal anatomical mapping of subcortical regions in Marmoset monkeys using high-resolution MRI and matched histology with multiple stains. Neuroimage. 2023; 281: 120311. *http://dx.doi.org/10.1016/j.2023.120311.*
3. Özarslan E, Koay CG, Shepherd TM, Komlosh ME, İrfanoğlu MO, Pierpaoli C, Basser PJ. Mean apparent propagator (MAP) MRI: a novel diffusion imaging method for mapping tissue microstructure. Neuroimage. 2013; 78:16-32.
4. Avram A, Sarlls JE, Barnett AS, Özarslan E, Thomas C, Irfanoglu MO, Hutchinson E, Pierpaoli C, Basser PJ. Clinical feasibility of using mean apparent propagator (MAP) MRI to characterize brain tissue microstructure. Neuroimage. 2016; 127:422-434.
5. Tournier JD, Calamante F, Connelly, A. MRtrix: diffusion tractography in crossing fiber regions. International journal of imaging systems and technology. 2012; 22:53-66.
6. Cox RW (1996). AFNI: software for analysis and visualization of functional magnetic resonance neuroimages. Comput Biomed Res 29 (3):162-173.
7. Taylor PA, Reynolds RC, Glen DR (2024). Improving skullstripping and nonlinear warping in AFNI: sswarper2. Presented at the 30th Annual Meeting of the Organization for Human Brain Mapping.
8. Fonov V, Evans AC, Botteron K, Almli CR, McKinstry RC, Collins DL, et al. Unbiased average age-appropriate atlases for pediatric studies. Neuroimage. 2011; 54, 313–327.
9. Wang F, Dong Z, Tian Q, Liao C, Fan Q, Hoge WS, Keil B, Polimeni JR, Wald LL, Huang SY, Setsompop K. In vivo human whole-brain Connectom diffusion MRI dataset at 760 µm isotropic resolution. Scientific Data. 2021; 8:1-12.
10. Amunts K, Lepage C, Borgeat L, Mohlberg H, Dickscheid T, Rousseau M, Bludau S, Bazin P, Lewis LB, Oros-Peusquens A, Shah NJ, Lippert T, Zilles K, Evans AC. BigBrain: An Ultrahigh-Resolution 3D Human Brain Model. Science. 2013; 340: 1472-1475.
11. Pajevic S, Pierpaoli C. Color schemes to represent the orientation of anisotropic tissues from diffusion tensor data: application to white matter fiber tract mapping in the human brain. Magn Reson Med. 1999; 42:526-540.

Support: Intramural Research Program of the *Eunice Kennedy Shriver* NICHD/NIH; Connectome 1.0: Developing the next-generation human MRI scanner for bridging studies of the micro-, meso- and macro-connectome, NIH BRAIN Initiative 1U01EB026996-01.